Springer

Journal of Mechanical Science and Technology 22 (2008) 1451~1459

Journal of Mechanical Science and Technology

www.springerlink.com/content/1738-494x
DOI 10.1007/s12206-008-0421-x

Structural integrity assessment of reactor pressure vessels during pressurized thermal shock

Myung Jo Jhung[1,*], Seok Hun Kim[1], Young Hwan Choi[1], Sunggyu Jung[2], Jong Min Kim[2], Ji Ho Kim[3], Jong Wook Kim[3], Changheui Jang[4], Yoon Suk Chang[5] and Ki Sig Kang[6]

[1]*Korea Institute of Nuclear Safety 19 Guseong-dong, Yuseong-gu, Daejeon 305-338, Korea*
[2]*Korea Power Engineering Company*
[3]*Korea Atomic Energy Research Institute*
[4]*Korea Advanced Institute of Science and Technology*
[5]*Sungkyunkwan University*
[6]*International Atomic Energy Agency*

(Manuscript Received June 4, 2007; Revised February 26, 2008; Accepted April 23, 2008)

Abstract

A comparative assessment study is performed for the deterministic fracture mechanics approach of the pressurized thermal shock of a reactor pressure vessel. Round robin problems consisting of two transients and two defects are solved. Their results are compared to suggest some recommendations of best practices and to assure an understanding of the key parameters of this type of approach, which will be helpful not only for the benchmark calculations and results comparisons but also as a part of the knowledge management for the future generation. Seven participants from five organizations solved the problem and their results are compiled in this study.

Keywords: Pressurized thermal shock; Reactor pressure vessel; Structural integrity; Warm prestressing

1. Introduction

At present, several different procedures and approaches are used for integrity assessment of reactor pressure vessels (RPVs). This is the case not only between eastern and western types of reactors but also within each group. These differences are based, in principle, on different codes and rules used for design, manufacturing and materials used for the various types of reactors on one side, and on the different level of implementation of recent developments in fracture mechanics on the other side. It is also the main reason why results from calculations of pressurized thermal shock (PTS) in different reactors cannot be directly compared.

Moreover, with the objective of assuring sufficient safety of operating reactors, the pressure has been increased to demonstrate proper integrity and lifetime evaluation of eastern reactor components. Several research projects aimed at improving the reliability of PTS analysis have been organized by international organizations; IAEA [1], OECD/NEA/CSNI [2-4] and EURATOM [5].

Based on existing activities, primarily qualitative results have been obtained from comparisons of different computer programs and analysis procedures. Such results are not sufficient to allow for a more detailed discussion and evaluation of safety margins implemented by the different computer programs and analysis procedures. Moreover, the developments in and applications of fracture mechanics are still evolving, while different computer programs contain different levels of application of more recent fracture

*Corresponding author. Tel.: +82 42 868 0467, Fax.: +82 42 861 9945
E-mail address: mjj@kins.re.kr

mechanics approaches, which also leads to some differences in results.

Several parameters are important in the RPV integrity evaluation during PTS, but they are defined and implemented in individual computer programs in different ways and to varying degrees depending on the overall approach used in the procedure. The approach is basically connected with the principal material fracture toughness approach as well as the implementation of further detailed inputs for the calculations.

Thus, benchmark calculation of the same typical PTS regime using different procedures and approaches with the same geometric, thermal-hydraulic, and material data is a good tool to compare results and to assess the effects of the individual input parameters on the final integrity evaluation.

In this study, comparative calculations of a typical PTS regime are performed by using different procedures and approaches with the aim to evaluate effects of individual parameters on the final RPV integrity evaluation. Also analyzed in this study are results from individual calculations with respect to the effects of the different procedures and approaches on the final maximum allowable transition temperature.

2. Problem definition

2.1 Reactor vessel

The reactor vessel considered in the analysis is a typical 3-loop western type of reactor, which is made of ASTM A 508 CL. 3 with an inner surface radius of 1994 mm, a base metal thickness of 200 mm, a cladding thickness of 7.5 mm and an outer surface radius of 2201.5 mm.

The postulated defect as a base case is a through-clad surface-breaking semi-elliptical crack of 19.5 mm depth × 117 mm length for $a'/c = 1/3$ as shown in Fig. 1. The orientation is axial in the weld metal and pressure is assumed to be applied on the crack face.

2.2 Transient

Two overcooling transients due to assumed leaks are defined as in Fig. 2, for which axisymmetric loading conditions are assumed. One is a typical PTS transient with repressurization. At the beginning of the transient, temperature and pressure decrease, but at a certain time, about 7200 s after the transient begins, the system pressure increases rapidly and slow heating occurs, and then temperature and pressure maintain nearly constant value. In this case, pressure may be a dominant factor. The other is a small break loss of coolant accident (SBLOCA). The temperature and pressure decrease very rapidly as shown in Fig. 2

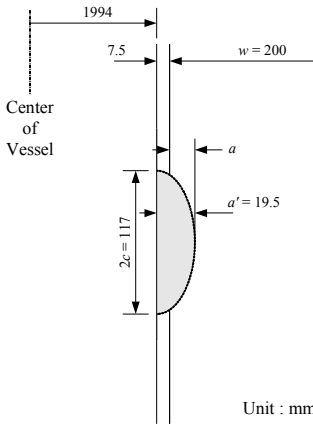

Fig. 1. Postulated defect

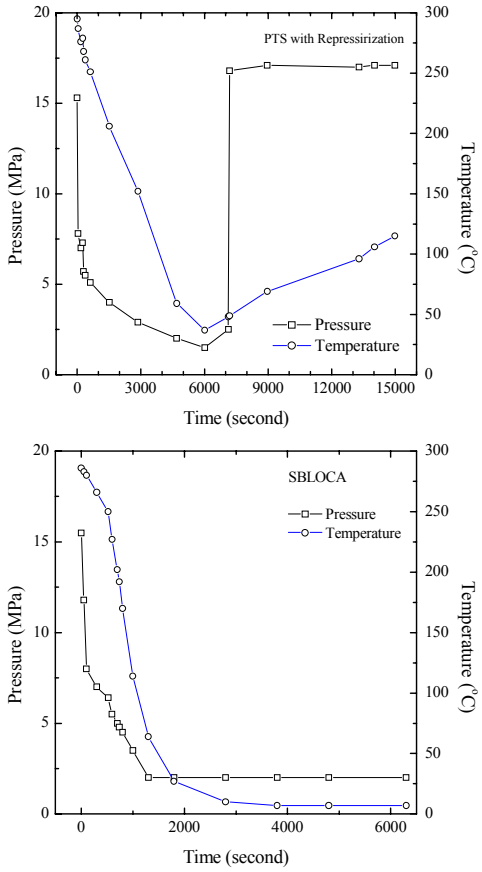

Fig. 2. Transient histories

and the final values are 7°C and 2 MPa, respectively. This transient has no repressurization as characterized by typical PTS transient. Therefore, it is expected that the temperature is a major factor to affect the results.

2.3 Sensitivity study

Several parametric studies can be proposed to investigate the influence of certain parameters on the results. Of these considered here are defect orientation (Table 1) and cladding material properties. The effect of cladding is investigated for three cases of crack number D1 as follows:

• C1 : No cladding. Cladding properties are assumed as identical to the base metal.

• C2 : Cladding thermal conductivity is considered. Additional stress from steep temperature gradient in cladding is evaluated.

• C3 : Cladding is fully considered. Additional stresses from steep temperature gradient and differential thermal expansion are evaluated.

3. Analysis

3.1 Analysis method

If a crack with a specific size and shape is given, it is necessary to check whether it is initiated or not during the PTS transient. In this study, the deepest point of a crack was investigated for possible initiation. The temperature and stress intensity factor histories at crack tip are calculated. Also, the fracture toughness K_{IC} is determined by using Eq. (1) with $K_{IC\ \max}$ = 220 MPa$\sqrt{\text{m}}$ for the variations of nil-ductility reference temperature (RT_{NDT}) [6] which is assumed arbitrarily.

$$K_{IC} = 36.5 + 22.783 \exp [0.036 (T - RT_{NDT})] \quad (1)$$

The upper bound of allowable RT_{NDT} is determined when the K_{IC} curve meets K_I curve tangentially, which is called tangent criterion (Fig. 3). In the same way, the upper bound of allowable RT_{NDT} is determined when K_{IC} curve intersects a maximum point of K_I curve, which considers a warm prestressing effect and is called maximum criterion. Even though the RT_{NDT} of the material is higher than the upper bound determined by the tangent criterion, the crack will not be initiated due to warm prestressing effect if it is lower than the upper bound determined by the maximum criterion. Therefore, the range of allowable RT_{NDT} is determined by two criteria, tangent criterion and maximum criterion, depending on the warm prestressing effect [7, 8].

Table 1. Analysis matrix for sensitivity study of postulated defect.

Crack Number	Location	Orientation	Shape	Aspect ratio (a'/c)	Depth	
					a	a/w
D1	surface	axial	semi-elliptical	1/3	12	0.06
D2	surface	circum.	semi-elliptical	1/3	12	0.06

3.2 Participants

Seven participants from five organizations presented the results. Participants represent all parties interested in the PTS analysis such as industry, research institute and regulatory body in Korea (Table 2). Participants that provided analysis results are identified only by a numeric code in the tables and comparative plots. This identification approach preserves anonymity of the contributing participants regarding analysis results. The computer codes and approaches employed by the participants are summarized in Table 3, which are subdivided into structural analysis, fracture analysis and model used. Most of participants employed finite element method using commercial codes for the structural analyses as shown in Table 3. The other participants used their own PTS-purpose computer codes employing analytical method.

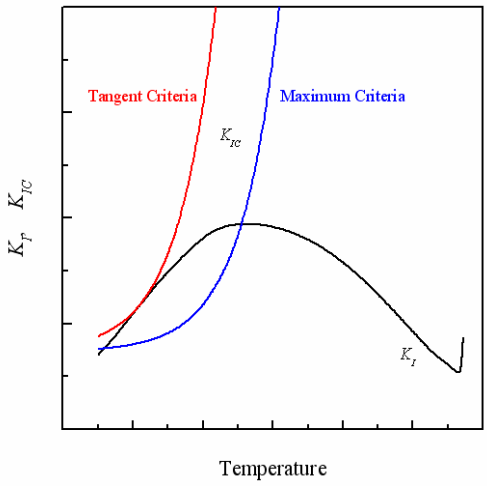

Fig. 3. Determination of maximum allowable RT_{NDT}.

Table 2. Organizations participating in the analysis.

Organization	E-mail
Korea Institute of Nuclear Safety	mjj@kins.re.kr, altong@kins.re.kr
Sungkyunkwan University	yschang7@skku.edu
Korea Advanced Institute of Science and Technology	chjang@kaist.ac.kr
Korea Atomic Energy Research Institute	jhkim12@kaeri.re.kr, kjwook@kaeri.re.kr
Korea Power Engineering Company	csg@kopec.co.kr, jmkim5@kopec.co.kr

Table 3. Comparison of analysis method and tools.

Participant No.	Analysis			Model
	Temperature	Stress	Fracture mechanics	
P1	Analytical	Analytical	Influence coefficient method	1-D
P2	ABAQUS	ABAQUS	Influence coefficient method	2-D
P3	ANSYS	ANSYS	Influence coefficient method	2-D
P4	ABAQUS	ABAQUS	Energy release method	3-D
P5	FEM	Analytical	Influence coefficient method	1-D
P6	ABAQUS	ABAQUS	Energy release method	3-D
P7	FAVOR	FAVOR	Influence coefficient method	1-D

Five participants out of seven used the influence coefficient method to calculate the stress intensity factor. One of the reasons for the large scatter in the stress intensity factors between participants may be the use of different influence coefficients.

4. Results and discussion

The maximum allowable transition temperature RT_{NDT}s determined by maximum criterion considering warm prestressing effect is shown in Fig. 4. As shown in some cases, there is a little scatter between participants, which is expected due to the different analysis method and/or different input parameters. For example, participants using influence coefficient method to calculate stress intensity factor employed different coefficients, resulting in a difference in stress intensity factor and also maximum allowable RT_{NDT} between participants.

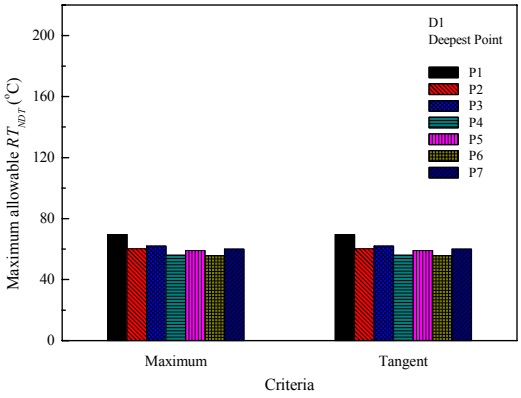

Fig. 4. Comparison of maximum allowable RT_{NDT}s by two criteria.

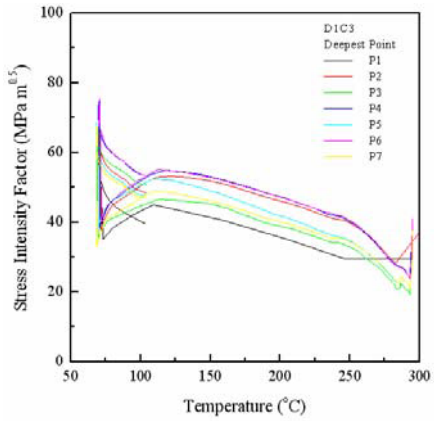

Fig. 5. Stress intensity factors with respect to temperature for D1C3.

The maximum allowable RT_{NDT} s determined by tangent criterion are also shown in Fig. 4. The stress intensity factors are plotted with respect to the temperature in Fig. 5, from which it is assumed that maximum and tangent criteria give the same allowable RT_{NDT} s for most cases. For the PTS transient with sudden repressurization as shown in Fig. 2, the benefit due to the warm prestressing effect for the crack initiation is not expected.

To perform fracture analysis for a crack in a reactor vessel wall, the time history of stress distribution in the vessel wall due to the temperature and pressure transient should be estimated. The stress distribution along the vessel wall at each time step should be approximated to a 3rd order polynomial equation to obtain the stress intensity factor [6]. However, the

stress intensity factor obtained by this method varies according to how the stress profile in the vessel wall is approximated because of the stress difference between the clad region and base metal region. Therefore, a stress approximation should be carefully carried out considering the stress profile in both the clad and base metal [9].

Even though a stress discontinuity exists between the clad and the base metal, the stresses in the clad and base metal are used together to calculate the stress intensity factor in the influence coefficient method. However, a participant, designated P2, used the stresses in the clad and the base metal separately to overcome the stress discontinuity [10]. First, the stress in the base metal is normalized through the wall thickness including the clad. Second, the clad stress difference between the normalized stress and the original stress is represented by using a linear expression (an equation of the first degree). And, the stress coefficients obtained from the first and second method are used to get the stress intensity factor.

Meanwhile, participant P5 used a different approach to calculate the stress intensity factor [11]. P5 calculated the stresses from various sources, such as thermal, pressure and residual stresses. P5 further divided the thermal stress components into clad stress confined within the narrow cladding and base stress. The stress intensity factor components calculated for the stress components are added to be the stress intensity factor at the crack tip. In this approach, the uncertainty associated the stress approximation can be avoided.

Participants P4 and P6 obtained stress intensity factors by converting the resulting *J*-integral with the following equation representing the plane strain condition:

$$K_I = \sqrt{\frac{JE}{1-\nu^2}} \tag{2}$$

Temperature and stress intensity factor histories at crack tip from participants are compared in Figs. 6 and 5, respectively. The temperature is almost the same at crack tip but the stress intensity factors have some differences among participants. The temperature distributions along the vessel wall at 3600 s and 7200 s are shown in Fig. 7 and they are similar, resulting in almost the same thermal stress between participants. The stress distributions along the vessel wall at the same instants are also shown in Fig. 8, which are very similar between participants except P4 which is lower than other participants by about 40 MPa at 7200 s. P4 calculates stresses from the 3-dimensional finite element model with crack and the stresses are obtained at the region which is away from crack and does not have end cap effect. Even though the stresses are the same, the methods to calculate the stress intensity factor are different as shown in Table 3, generating some differences among participants. Also, input parameters for deterministic approaches among participants are a little bit different. This may be a major factor to affect the results for determining the maximum allowable RT_{NDT}s. The effect of cladding is evaluated for three cases and the maximum allowable RT_{NDT}s are shown in Fig. 9, where considering cladding fully gives the most conservative results for all participants.

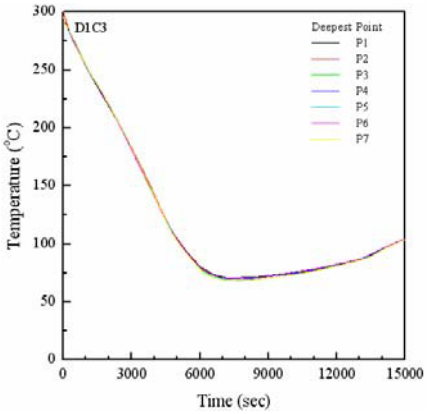

Fig. 6. Comparison of temperature variations.

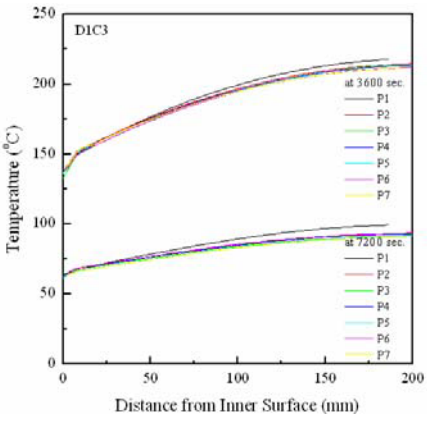

Fig. 7. Variation of temperature through the RPV wall thickness.

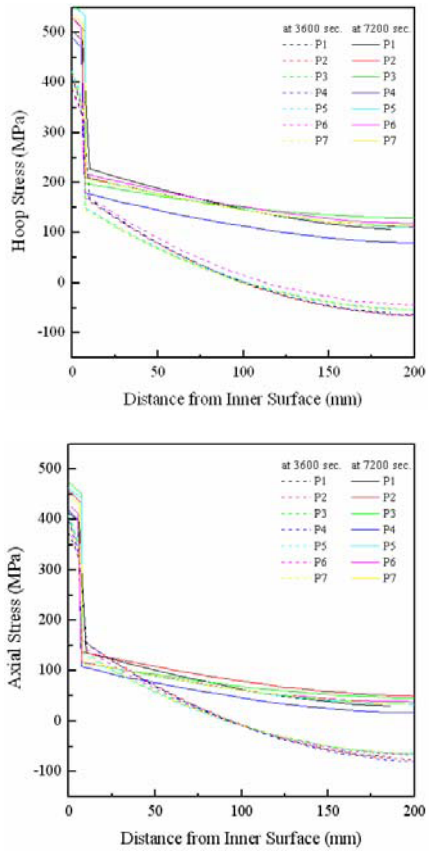

Fig. 8. Variation of stresses through the RPV wall thickness.

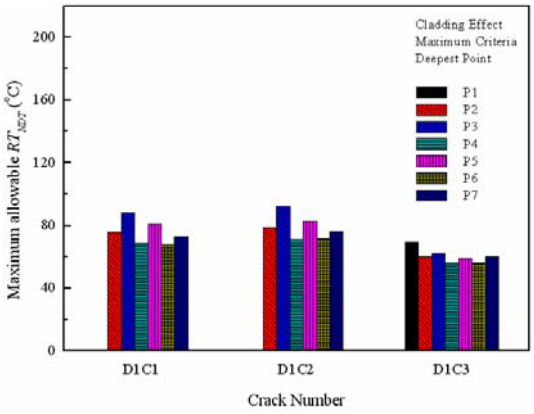

Fig. 9. Effect of cladding on maximum allowable RT_{NDT}.

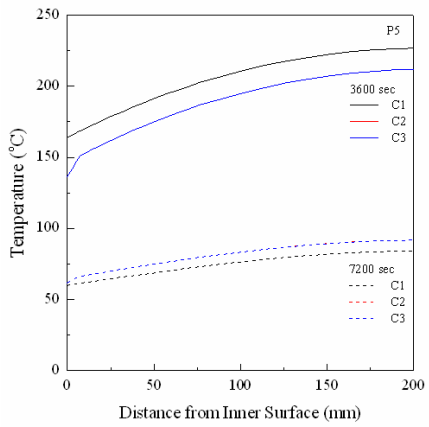

Fig. 10. Comparison of temperature profiles within vessel.

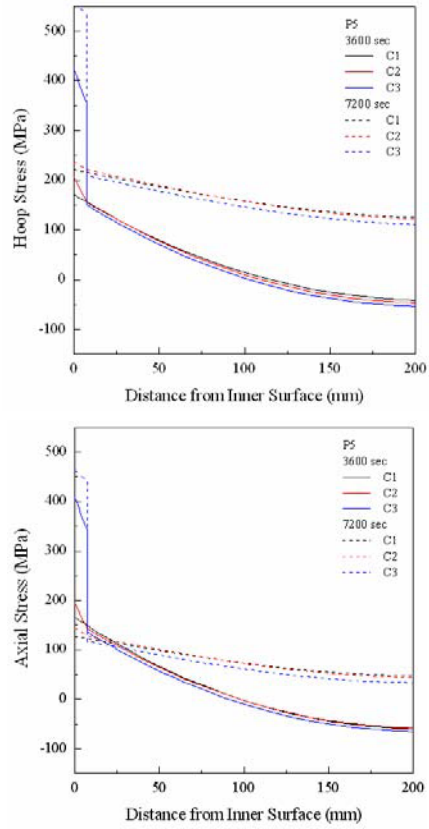

Fig. 11. Comparison of stress profiles within vessel.

Temperature profiles within the RPV at 3600 s and 7200 s into the transient are shown in Fig. 10. As expected when the cladding thermal conductivity was considered (C2 and C3), the temperature within the base metal region at 7200 s increased about 5ºC compared to that when it was neglected. Because the material resistance to fracture increased exponentially with the temperature, such temperature differences could have large effect on the material resistance to the flaw initiation.

The hoop and axial stress profiles are shown in Fig. 11. Unlike the temperature C1 and C2 produced simi-

lar stress profiles suggesting that considering the thermal conductivity alone had not so significant effects on the hoop stress profile. Within the cladding, the hoop stress was the largest when both the thermal conductivity and the thermal expansion of the cladding were considered. By comparing C2 and C3, it was clear that the effect of the cladding thermal expansion was far greater than that of the cladding thermal conductivity.

The resulting stress intensity factors at the crack tip of the semi-elliptical surface crack are shown in Fig. 12. As for the hoop stress, C1 and C2 produced about the same stress intensity factors. However, C3 showed the largest stress intensity factor at the crack tip because of the high tensile stress within the cladding region. The differences are greater near the cladding/base interface where the effect of cladding stress was dominant and gradually decreased.

From the above results, it was expected that considering the low thermal conductivity of cladding alone (C2) would result in the least conservative analysis results. Also, the maximum allowable RT_{NDT}s for crack initiation were highest when only the cladding thermal conductivity was considered, and lowest when both the cladding thermal conductivity and thermal expansion were considered in the analysis.

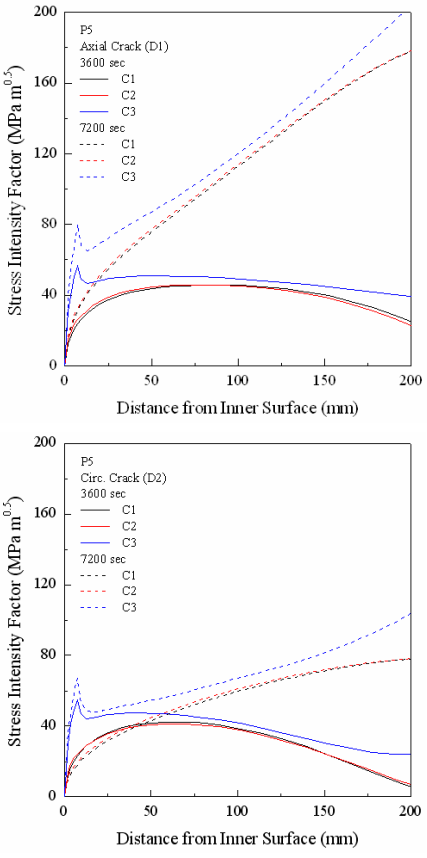

Fig. 12. Comparison of stress intensity factor profiles within vessel.

The effect of defect orientation is investigated for the axial and circumferential directions. The maximum allowable RT_{NDT}s are shown in Fig. 13, which shows that the allowable RT_{NDT} for circumferential crack is much higher than that of axial one by about 60°C. From the stress intensity factor variation as a function of temperature for circumferential crack D2 (Fig. 14), the lowest allowable RT_{NDT}s are expected for P3 because it has the highest stress intensity factors but it is too low as shown in Fig. 13. Two peaks appeared in the stress intensity plot at around 4500 s and 7200 s and the maximum stress intensity factor is obtained at the first peak by all participants except P3. The determination of the allowable RT_{NDT}s at two peaks may be exampled for P6 as shown in Fig. 15 by maximum and tangent criteria. As shown in Fig. 15, the difference of the stress intensity factor at two points is not big but that of the allowable RT_{NDT}s is very big. That's because the temperature difference at 4500 s and 7200 s is about 50°C resulting in the big fracture toughness differences. P3 obtained the allowable RT_{NDT}s by maximum criterion at around 7200 s but the others at around 4500 s. That's why there is a large difference between P3 and other participants. Except for P3 which has a peak stress intensity factor at 7200 s differently from others, P1 has the lowest allowable RT_{NDT} as expected because it has the largest stress intensity factors. But the allowable RT_{NDT}s by tangent criteria are obtained at around 7200 s by all participants and are on the order of the magnitude of stress intensity factors at around 7200 s as shown in Fig. 13. Therefore, it is recommended to consider the time of crack initiation as well as the maximum allowable RT_{NDT} in the comparison of evaluation results. This is a good example to show that the maximum criterion is not reasonable in some cases and is very sensitive to the results. Even though the stress intensity factor of P3 does not differ from others significantly as shown in Fig. 14, the difference in allowable RT_{NDT} by maximum criteria is very big.

The allowable RT_{NDT} for SBLOCA is 55.5°C by tangent criterion, which is comparable to the 55.7°C for PTS. Even though the difference of maximum stress intensity factor between PTS and SBLOCA is

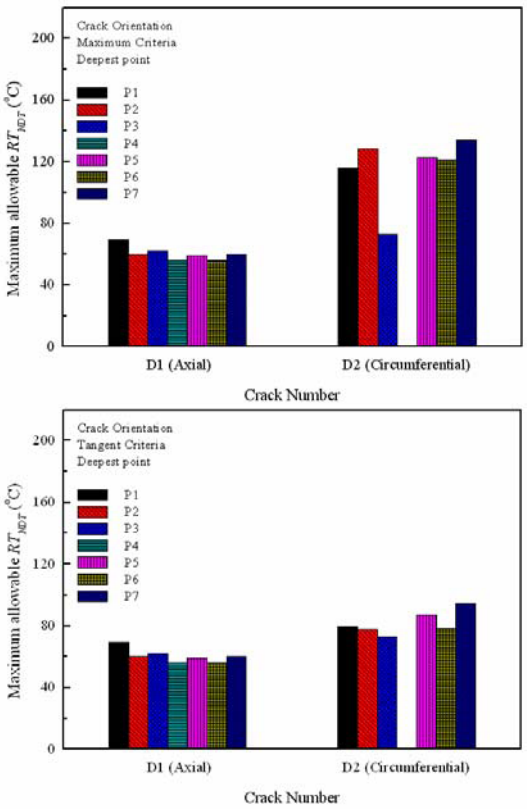

Fig. 13. Effect of defect orientation on maximum allowable RT_{NDT}.

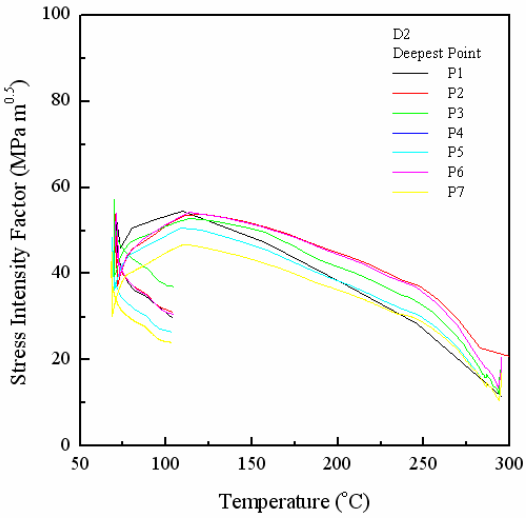

Fig. 14. Stress intensity factors for D2.

about 22 MPa·m$^{0.5}$, the allowable RT_{NDT} is almost the same, which is caused by the time when the initiation occurs and the temperature at that instant. The allowable RT_{NDT} is 101.2°C by maximum criterion, which is comparable to the 55.7°C for PTS. By comparison of the allowable RT_{NDT} between PTS and SBLOCA, it is clear that warm prestressing is very effective in the SBLOCA which has a rapid cooling and depressurization without repressurization. In this case, the warm prestressing benefits of allowable RT_{NDT}s are 45.7°C and 32.5°C at the deepest and 2 mm below interface points, respectively.

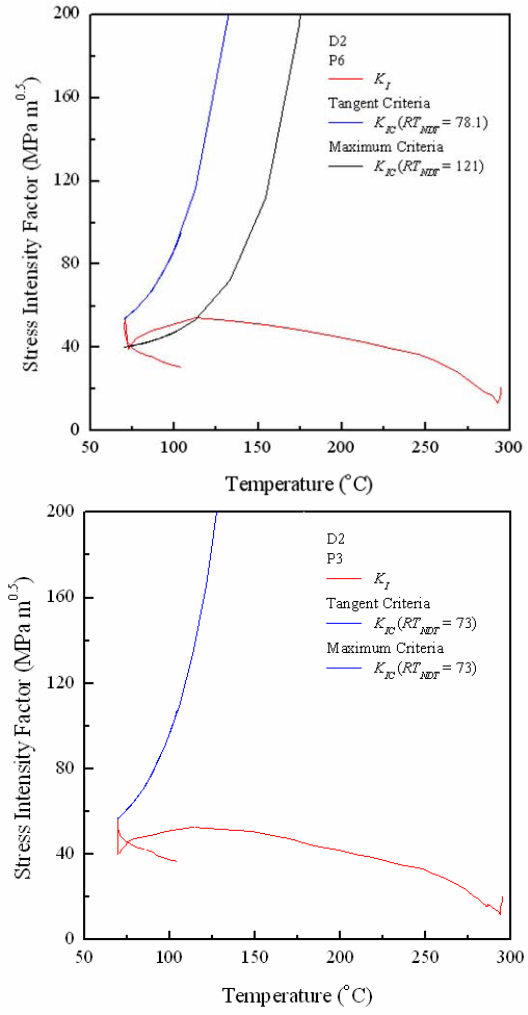

Fig. 15. Determination of allowable RT_{NDT}s by maximum and tangent criteria.

5. Conclusions

Round robin analyses of the reactor pressure vessel under the pressurized thermal shock are performed. Two transients and two defects are postulated and the

deterministic fracture mechanics analyses are performed to determine the maximum allowable RT_{NDT}s. Results from participants are compared generating following conclusions:

• The calculated maximum allowable RT_{NDT}s have the scatter differing among participants, which is apparently caused by the difference of stress intensity factors among participants and the selection of different input parameters for analysis.

• When the differences in thermal conductivity and thermal expansion coefficients of cladding are fully considered, the stress intensity factor increases, which is greater near the cladding/base interface resulting in the decrease of the maximum allowable RT_{NDT}. Considering cladding thermal conductivity alone produces the most unconservative allowable RT_{NDT}.

• The time of crack initiation as well as the maximum allowable RT_{NDT} is a very important factor to be considered in the PTS evaluation.

• SBLOCA is more severe than PTS with repressurization by tangent criteria but when considering warm prestressing PTS with repressurization is more severe than SBLOCA. The benefit of the allowable RT_{NDT} due to a warm prestressing effect is apparent to SBLOCA where system repressurization does not occur.

References

[1] IAEA, *Guidelines on pressurized thermal shock analysis for WWER nuclear power plants*, IAEA-EBP-WWER-08, Rev.1, International Atomic Energy Agency, Vienna, (2005).

[2] J. Sievers and B. R. Bass, Comparative assessment of project FALSIRE - results, *Nuclear Engineering and Design*, 152 (1994) 19-37.

[3] B. R. Bass, C. E. Pugh, J. Sievers and H. Schulz, Overview of the International Comparative Assessment Study of Pressurized Thermal Shock in Reactor Pressure Vessels (RPV PTS ICAS), *The International Journal of Pressure Vessels and Piping*, 78 (2001) 197-211.

[4] C. Faidy, PROSIR – Probabilistic Structural Integrity of a PWR Reactor Pressure Vessel, Proposed to OECD/NEA PWG3 – Metal Group, EDF-SEPTEN, (2003).

[5] D. P. G Lidbury, A. H. Sherry, B. R. Bass, P. Gilles, D. Connors, U. Eisele, E. Keim, H. Keinanen, K. Wallin, D. Lauerova, S. Marie, G. Nagel, K. –F. Nilsson, D. Siegele and Y. Wadier, Validation of Constraint-Based Methodology in Structural Integrity of Ferritic Steels for Nuclear Reactor Pressure Vessels, *Fatigue and Fracture of Engineering Materials and Structures*, 29 (2006) 1-21.

[6] ASME, ASME Boiler and Pressure Vessel Code, Section XI Rules for Inspection of Nuclear Power Plant Components, Appendix A Analysis of Flaws, The American Society of Mechanical Engineers, (2004).

[7] M. J. Jhung, Y. W. Park and C. Jang, Pressurized Thermal Shock Analyses of a Reactor Pressure Vessel Using Critical Crack Depth Diagrams, *The International Journal of Pressure Vessels and Piping*, 76 (12) (1999) 813-823.

[8] M. J. Jhung, S. H. Kim, J. H. Lee and Y. W. Park, Round robin analysis of pressurized thermal shock for reactor pressure vessel, *Nuclear Engineering and Design*, 226 (2003) 141-154.

[9] M. J. Jhung, C. Jang, S. H. Kim, Y. H. Choi, H. J. Kim, S. G. Jung, J. M. Kim, G. H. Sohn, T. E. Jin, T. S. Choi, J. H. Kim, J. W. Kim and K. B. Park, Round robin analysis for probabilistic structural integrity of reactor pressure vessel under pressurized thermal shock, *Journal of Mechanical Science and Technology*, 19 (2) (2005) 642-656.

[10] S. Marie, Y. Menager and S. Chapuliot, Stress intensity factors for underclad and through clad defects in a reactor pressure vessel submitted to a pressurized thermal shock, *International Journal of Pressure Vessels and Piping*, 82 (2005) 746-760.

[11] C. Jang, S. C. Kang, H. R. Moonn, I. S. Jeong and T. R. Kim, The Effects of the Stainless Steel Cladding in Pressurized Thermal Shock Evaluation, *Nuclear Engineering and Design,* 226 (2003) 127-140.